Geophysical Research Letters

RESEARCH LETTER
10.1029/2020GL091543

Tibetan Plateau Precipitation Modulated by the Periodically Coupled Westerlies and Asian Monsoon

Anning Cui[1,2], Houyuan Lu[1,2,3], Xingqi Liu[4,5], Caiming Shen[6], Deke Xu[1,2,3], Baiqing Xu[7,8], and Naiqin Wu[1,2,3]

[1]Key Laboratory of Cenozoic Geology and Environment, Institute of Geology and Geophysics, Chinese Academy of Sciences, Beijing, China, [2]University of Chinese Academy of Sciences, Beijing, China, [3]Innovation Academy for Earth Science, Chinese Academy of Sciences, Beijing, China, [4]College of Resource Environment and Tourism, Capital Normal University, Beijing, China, [5]State Key Laboratory of Lake Science and Environment, Nanjing Institute of Geography and Limnology, Chinese Academy of Sciences, Nanjing, China, [6]Yunnan Key Laboratory of Plateau Geographical Processes and Environmental Changes, College of Tourism and Geographical Sciences, Yunnan Normal University, Kunming, China, [7]Key Laboratory of Tibetan Environment Changes and Land Surface Processes, Institute of Tibetan Plateau Research, Chinese Academy of Sciences, Beijing, China, [8]Centre for Excellence in Tibetan Plateau Earth Sciences, Chinese Academy of Sciences, Beijing, China

Abstract Knowledge of decadal-centennial-scale precipitation cycles is important for predicting the status of water resources and thus food security in the region influenced by the "Asian Water Tower" (the Tibetan Plateau, TP). However, the drivers of these precipitation cycles in the TP remain unclear. Here we present a 1,656-years (5-years-resolution) mean annual precipitation record reconstructed by fossil pollen assemblages from the annually laminated sediments of a lake in the TP interior. The record reveals three dominant cycles, with lengths of ~200-, ~88-, and ~60-years, associated with changes in the Westerlies and the Asian monsoon. These precipitation cycles suggest that the current high precipitation in the TP interior results from the superposition of cyclic highs in precipitation, and this trend may continue for the next several decades.

Plain Language Summary Humidification resulting from increased precipitation over the Tibetan Plateau interior has attracted widespread because although it improves the ecological environment but it also threatens the security of the Qinghai-Tibet Railway. Understanding the past behavior and mechanisms of precipitation variations over the Tibetan Plateau interior aids in the prediction of future water resource availability. We present a reconstruction of mean annual precipitation, derived from the pollen assemblages deposited in the annually laminated sediments of the Kusai Lake. The precipitation record exhibits three significant multidecadal-centennial cycles; the ~200-years cycle is associated with the Westerlies and the ~88-years and ~60-years cycles are linked with the Asian monsoon. The superposition of high phases of cyclic precipitation results in the current wetting trend in the Tibetan Plateau interior.

Anning Cui and Houyuan Lu contributed equally to this work.

Key Points:

- Precipitation reconstructed by lacustrine pollen assemblages from the Tibetan Plateau interior reveals three decadal-centennial oscillations
- The decadal and centennial cycles are closely related to the Westerlies and the Asian Monsoon, respectively
- Superimposition of cyclic precipitation highs may have been factors in the current regional wetting trend

Supporting Information:

- Supporting Information S1

Correspondence to:

H. Lu and A. Cui,
houyuanlu@mail.iggcas.ac.cn;
cuianning2016@mail.iggcas.ac.cn

Citation:

Cui, A., Lu, H., Liu, X., Shen, C., Xu, D., Xu, B., & Wu, N. (2021). Tibetan plateau precipitation modulated by the periodically coupled westerlies and Asian monsoon. *Geophysical Research Letters*, *48*, e2020GL091543. https://doi.org/10.1029/2020GL091543

Received 10 NOV 2020
Accepted 11 FEB 2021

1. Introduction

As the "Asian Water Tower", the Tibetan Plateau (TP) plays a crucial role in regulating the hydro-climatology of several prominent Asian rivers, which sustain more than one-fifth of the world's population in the neighboring countries (Immerzeel et al., 2010). In recent decades, the expansion of lake areas as well as the rise of lake levels resulting from increased precipitation and melting of glaciers have been observed in the TP interior (Lei et al., 2014; Zhang et al., 2019, 2017). The increased precipitation could substantially improve the ecological environment via increases in vegetation coverage and ecosystem productivity; however, it may also increase the risk of flood disasters threatening the Qinghai-Tibet Railway (Yao et al., 2012). Therefore, determining whether the precipitation increase across the TP is the result of decadal-centennial-scale precipitation cycles is important for predicting the future status of water resources and food security in the region (Immerzeel et al., 2010). In order to investigate the processes, trends, and mechanisms of precipitation variations in the TP interior, several short-term observational datasets and a small number of long-term precipitation records have been produced in the last 20 years.

Observational data indicate that the water vapor in the TP interior is mainly transported by the mid-latitude Westerlies and the South Asian summer monsoon (SASM, Wang et al., 2017a; Yao et al., 2013). However, observational data within the ~100-years interval in these studies is not long enough to reveal patterns of precipitation variability on the multidecadal-centennial scale. Although the available long-term precipitation records derived from tree-rings can extend as far as 3,500 years into the past (Yang et al., 2014), they are from the low-elevation marginal regions of the TP, where the water vapor is supplied by the East Asian summer monsoon (EASM, Shao et al., 2005) or the SASM (Overpeck et al., 2005; Yadav, 2011). Precipitation records spanning the past few centuries based on the accumulation rate of ice cores are also available from the high mountains in the TP, but the precipitation processes are quite different from those in the interior of the TP, although the water vapor in both cases is transported by the Westerlies and the Asian summer monsoon (Liu et al., 1998; Tian & Yao, 2016; Yao et al., 2013; Zhao et al., 2020). Therefore, long-term precipitation records from the TP interior are important for revealing precipitation cycles on the decadal-centennial scale and their driving mechanisms.

Given the wide distribution of lakes in the TP, lacustrine sediments are more suitable than the more geographically limited tree-ring and ice core records for reconstructing past variations in the hydroclimatic conditions of the TP interior. Many studies have used biotic and abiotic indicators from lake sediments as quantitative climatic proxies (Liu et al., 2014; Lu et al., 2011; Shen et al., 2006a). Among them, fossil pollen records from lakes have been widely used to reconstruct the paleoclimate of the TP interior. However, ^{14}C reservoir age effects are common within the lakes of the TP interior, which introduces uncertainty into spatial and temporal paleoclimatic reconstructions based on lacustrine records (Hou et al., 2012). Fortunately, however, a lake with annually laminated sediments has been discovered in the TP interior.

Here we present a 5-years-resolution quantitative mean annual precipitation (MAP) record of the past 1,656 years from the TP interior. The record is inferred based on pollen assemblages from the annually laminated sediments of Lake Kusai and was obtained using a weighted averaging partial least squares (WA-PLS) regression model. The record exhibits three significant multidecadal-centennial cycles, which acted synergistically to modulate precipitation variations in the TP interior. The relationships between these dominant multidecadal-centennial precipitation cycles and large-scale atmospheric circulation patterns can be used to interpret precipitation variability within the TP over the last 1,656 years. In addition, the results provide a context for interpreting recently increased precipitation across the TP, suggesting the possible persistence of high precipitation in the future.

2. Study Area

Kusai Lake (35.5°–35.8°N, 92.5°–93.25°E, 4,475 m) is a saline lake located in the uninhabited Hoh Xil region of the TP interior (Wang & Dou, 1998). The lake area is 254.4 km^2 and the catchment area is ~3,700 km^2. The lake is fed mainly by the Kusai River which enters the southwestern part of the basin. The regional precipitation is modulated by the mid-latitude Westerlies and the low-latitude Asian monsoon (Figure 1a, Zhang, 1992). Using NOAA's Hybrid Single-Particle Lagrangian Integrated Trajectory (HYSPLIT4, Draxler & Hess, 1997) model, we analyzed daily backward moisture trajectories of rainfall events at Kusai Lake. The moisture transported by the Westerlies accounts for 59% of the annual rainfall, whereas the water vapor transported by the SASM supplies ~29% of that (Figure S1).

Recent climatic data (1957–2006) from Wudaoliang Meteorological Station show that the MAP is ~278 mm and the mean annual temperature (MAT) is about −5.4°C. The catchment of Kusai Lake experiences an alpine climate with an interpolated MAP of 208 mm and an interpolated MAT of −3.3°C (Fick & Hijmans, 2017). These climatic characteristics result in the dominance of annual herbaceous vegetation across the Hoh Xil region. The vegetation around Kusai Lake is alpine steppe dominated by drought-resistant *Artemisia* and Poaceae, and alpine meadow dominated by hygrophilous Cyperaceae. In the northeast part of the lake catchment, xerophytic Chenopodiaceae are sporadically distributed (Figure 1b).

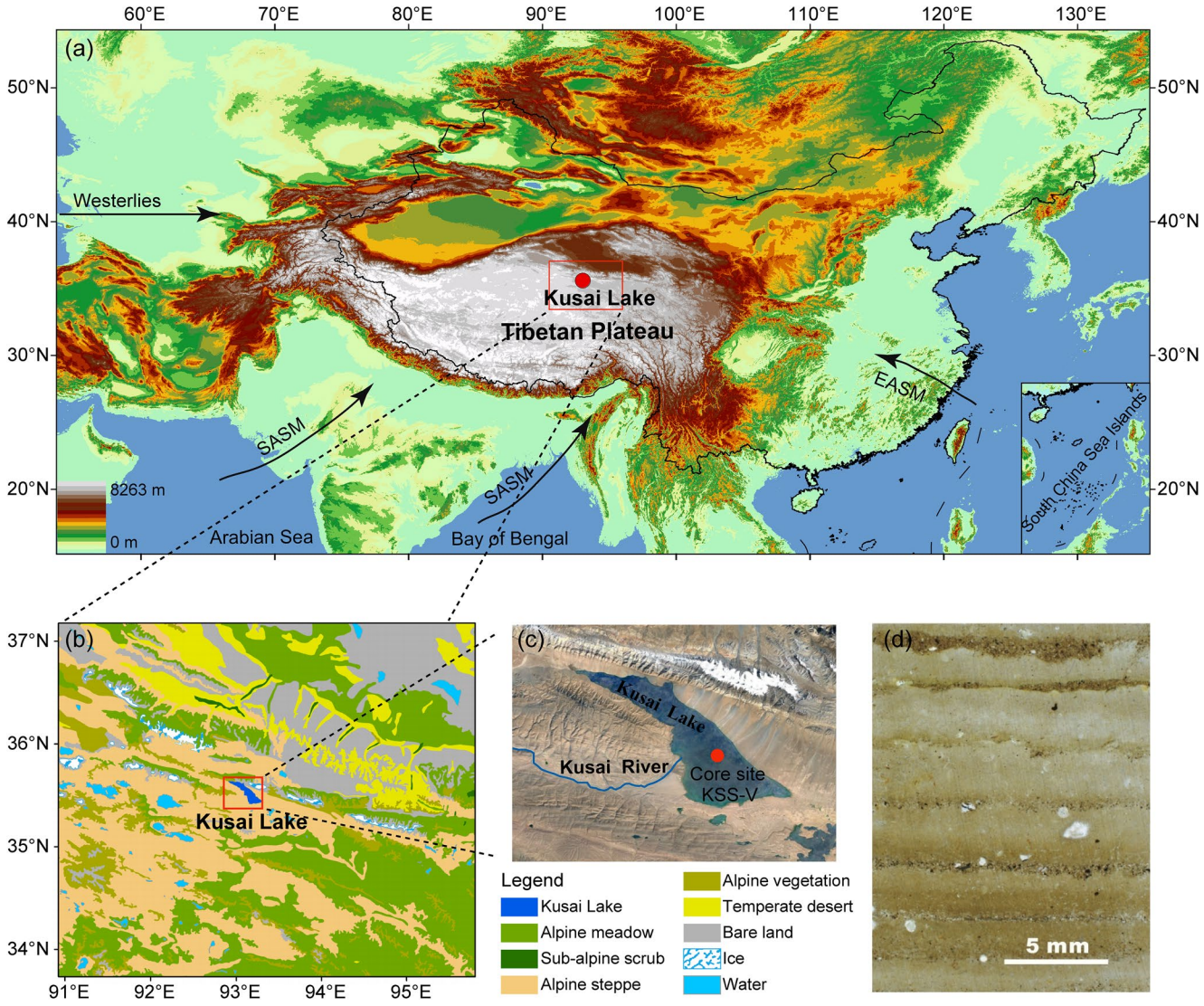

Figure 1. Location of Kusai Lake on various spatial scales. (a) Digital Terrain Model showing the location of Kusai Lake within Asia and schematic trajectories of the Westerlies, the SASM, and the EASM. (b) Vegetation types within study area (Zhang, 2007). (c) Screenshot of Kusai Lake from Google Earth. (d) Scanned images of the annually laminated sediment core (Liu et al., 2014). EASM, East Asian summer monsoon; SASM, South Asian summer monsoon.

3. Materials and Methods

3.1. Sediment Core

In September 2006, a 364-cm-long sediment core (KSS-V) was raised from the southeastern part of Kusai Lake in a water depth of 14.5 m (Figure 1c). The sediment core contains rhythmic dark and light layers throughout (Figure 1d). The dark units are formed by coarse sand and silt accumulating on the lake ice during winter. The light layers are composed of clay minerals accumulating during summer. The sediment core was cut into blocks for lamination counting. With the assistance of an optical microscope, we counted the lamination at least three times to determine an age model, which has a ~1% error based on replicate counts. Additionally, we measured the ^{210}Pb, ^{137}Cs activity of the upper 25 cm of the core and 11 AMS ^{14}C ages to validate the robustness of the age model based on annual laminations. Details of the age model are given in our previous study (Figure S2, Liu et al., 2014).

3.2. Pollen Analysis and Quantitative Paleoclimatic Reconstruction

364 samples with an average resolution of 5-years were used for pollen analysis. *Lycopodium* spores (27,560 grains/tablet) were used before acid-alkali treatment to calculate pollen concentrations. Sample residues were mounted in glycerin and analyzed using a Leica DM 750 microscope with the aid of the Pollen Flora of China (Tang et al., 2016). More than 400 terrestrial pollen grains were counted per sample. Pollen percentages were calculated based on the sum of total pollen grains and pollen diagrams were plotted using Tilia software (Grimm, 1987).

MAP and MAT were quantitatively reconstructed using C2 software (Juggins, 2003). The modern pollen dataset was derived from previous work (Lu et al., 2011). An optimal transfer function was selected by minimizing the root mean-square-error of prediction (RMSEP) and maximizing the coefficient of determination (R^2) between observed and predicted MAP values.

3.3. Statistical Analysis

In order to detect the dominant modes of the oscillations in the MAP, we first performed ensemble empirical mode decomposition (EEMD, Huang & Wu, 2008), a noise-assisted data analysis, on the reconstructed MAP. We then calculated the power spectrum of the detrended MAP using the Morlet wavelet to characterize its statistical significance (Schulz & Mudelsee, 2002; Torrence & Compo, 1998). Finally, we estimated the MAP for the next 50 years using singular spectrum analysis (SSA), a widely used nonparametric spectral estimation method in nonlinear climatic time series analysis (Golyandina & Korobeynikov, 2014), although its predictability is probably limited by stationary signals due to the enhancement of human activities in the recent past.

4. Results

4.1. Chronology

The age model spans 1,656 years (from 350 to 2006 AD) which is directly inferred from counting annual laminations, as previously described (Figure S2, Liu et al., 2014).

4.2. Pollen Record and Quantitative Reconstruction of MAP

A total of 62 pollen types were recognized in the samples (Figure S3). The pollen spectra are characterized by high percentages of herbaceous pollen (90%), mainly Chenopodiaceae, *Artemisia*, Cyperaceae, Poaceae, Caryophyllaceae, *Thalictrum*, and *Aster* (Figure 2a). All pollen types with relative abundances >2% in at least one sample were used for subsequent reconstruction. Numerical analysis of the 735 modern pollen samples and environmental parameters showed that MAP had the strongest correlation with the modern pollen spectra (Figures S4a–b, and Table S1), indicating that the modern pollen dataset can be used to establish pollen-climate transfer functions and hence a reliable quantitative reconstruction of MAP. In addition, the results of analogue analysis revealed all of the fossil pollen samples have good analogs within the training set (Figure S4c, Overpeck et al., 1985). Finally, an optimal transfer function established using the WA-PLS regression model (Braak & Juggins, 1993) was selected because it had the highest coefficient of determination ($R^2_{boot} = 0.76$) and the lowest RMSEP value (RMSEP = 68 mm, Juggins, 2003). Similarly, the optimal transfer function for MAT reconstruction was selected with the R^2_{boot} value equal of 0.62 and RMSEP of 2.44°C (Figures S4d–g and S5).

A comparison of reconstructed MAP values since 1960 AD which estimated from 13 fossil pollen spectra with observed MAP values (5-years moving averages) ($r = 0.89$, P-value <0.001), reveals a similar trend and validates the accuracy of the reconstructed MAP (Figure 2b). Notably, the observed MAP values are slightly higher than the reconstructed MAP since the MAP in the catchment of Kusai Lake is less than that at Wudaoliang Station. In addition, the reconstructed MAP commences a large increase since 1980 AD, as indicated by the observational data. Increased precipitation was probably the main reason for the overflowing of several lakes in the Hoh Xil region in 2011 AD (Yao et al., 2012), as well as for a general wetting trend across the TP interior. Therefore, the modern and fossil pollen data enable us to reliably reconstruct

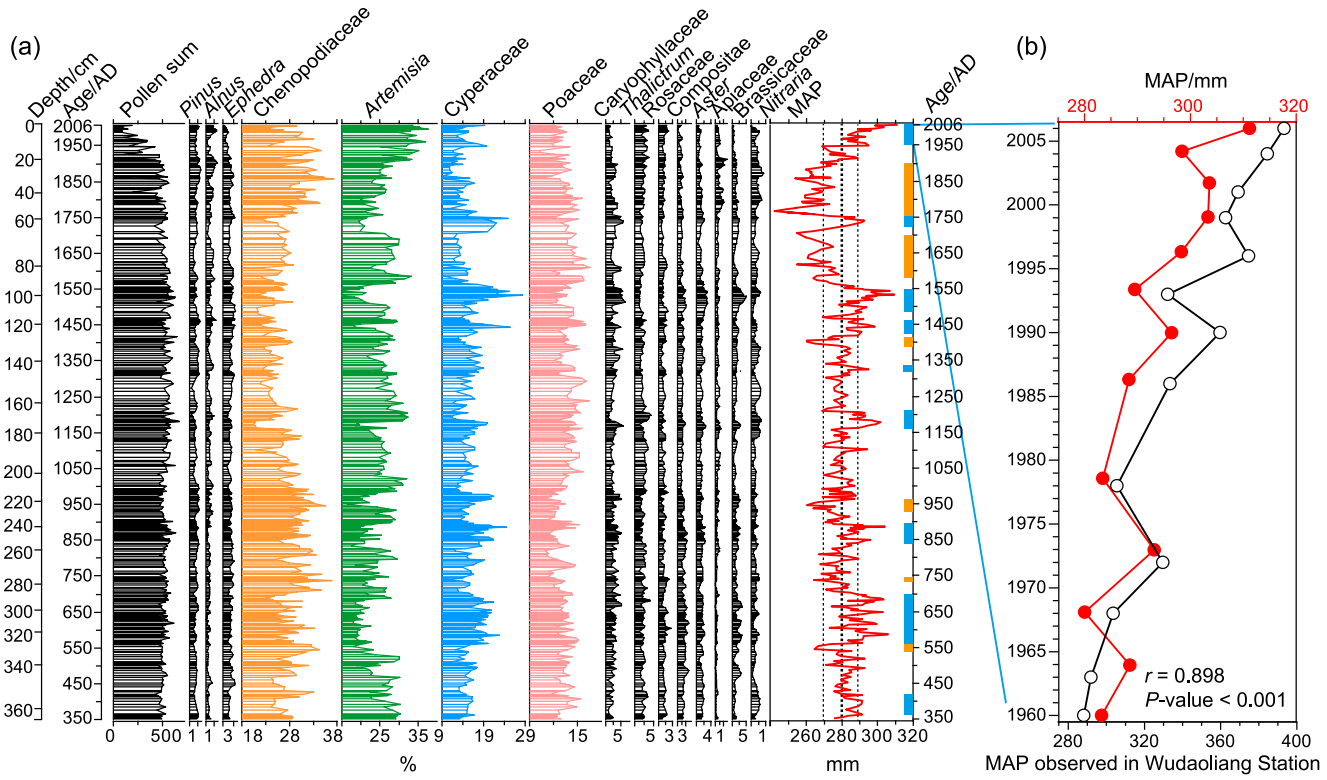

Figure 2. Pollen percentage diagram for Kusai Lake and comparison of reconstructed and observed MAP values. (a) Pollen percentage diagram for Kusai Lake and reconstructed MAP. The blue and yellow bars represent wet and dry periods, respectively. (b) Comparison of reconstructed MAP and observed MAP from Wudaoliang Meteorological Station. The red line with solid circles denotes the reconstructed MAP values during 1960–2006 AD, and the black line with open circles denotes the 5-years moving average of the observed MAP (Data from http://data.cma.cn).

the dynamics of the MAP in the TP interior. Here we also use one standard deviation of the MAP as the threshold to detect high and low precipitation intervals. The MAP record has an average of 279 mm and a standard deviation of 10 mm, and the periods with average precipitation above 289 mm are thus regarded as high precipitation intervals: 360–420, 560–700, 840–890, 1160-1210, 1320-1335, 1430-1460, 1490-1550, 1730-1750, and 1950–2006 AD. The periods with average precipitation less than 269 mm are low precipitation intervals: 540–560, 730–740, 930–960, 1390-1410, 1580-1700, and 1750–1900 AD. Notably, the reconstructed precipitation record is characterized by a series of oscillations.

Additionally, the most striking feature of the pollen record is the oscillations between hydrophilic Cyperaceae (constituents of alpine meadow) and drought-resistant *Artemisia* (a constituent of alpine steppe) as well as xerophytic Chenopodiaceae (constituents of alpine and temperate desert). The abrupt transitions between the Cyperaceae, *Artemisia*, and Chenopodiaceae phases reflect regional vegetation changes characterized by shifts between alpine meadow, steppe, and desert in the catchment of Kusai Lake, indicating corresponding shifts in regional precipitation. The high abundance of Cyperaceae indicates high precipitation intervals, whereas high abundances of *Artemisia* and Chenopodiaceae indicate low precipitation hence dry intervals. It is evident that the oscillations in the pollen record and reconstructed MAP are quasi-periodic but with different time-scales of fluctuation over the past 1,656 years.

4.3. Periodic Changes in the Pollen Record and Reconstructed MAP

Nine EEMD components (c1–c9) are shown in Figure 3a. Considering the duration and temporal resolution of the MAP record, we removed the long-term trend and decadal-scale noise and selected the sum c3–5 (c3 + c4 + c5) to precisely reproduce the information recorded in the MAP, which also showed clear oscillations.

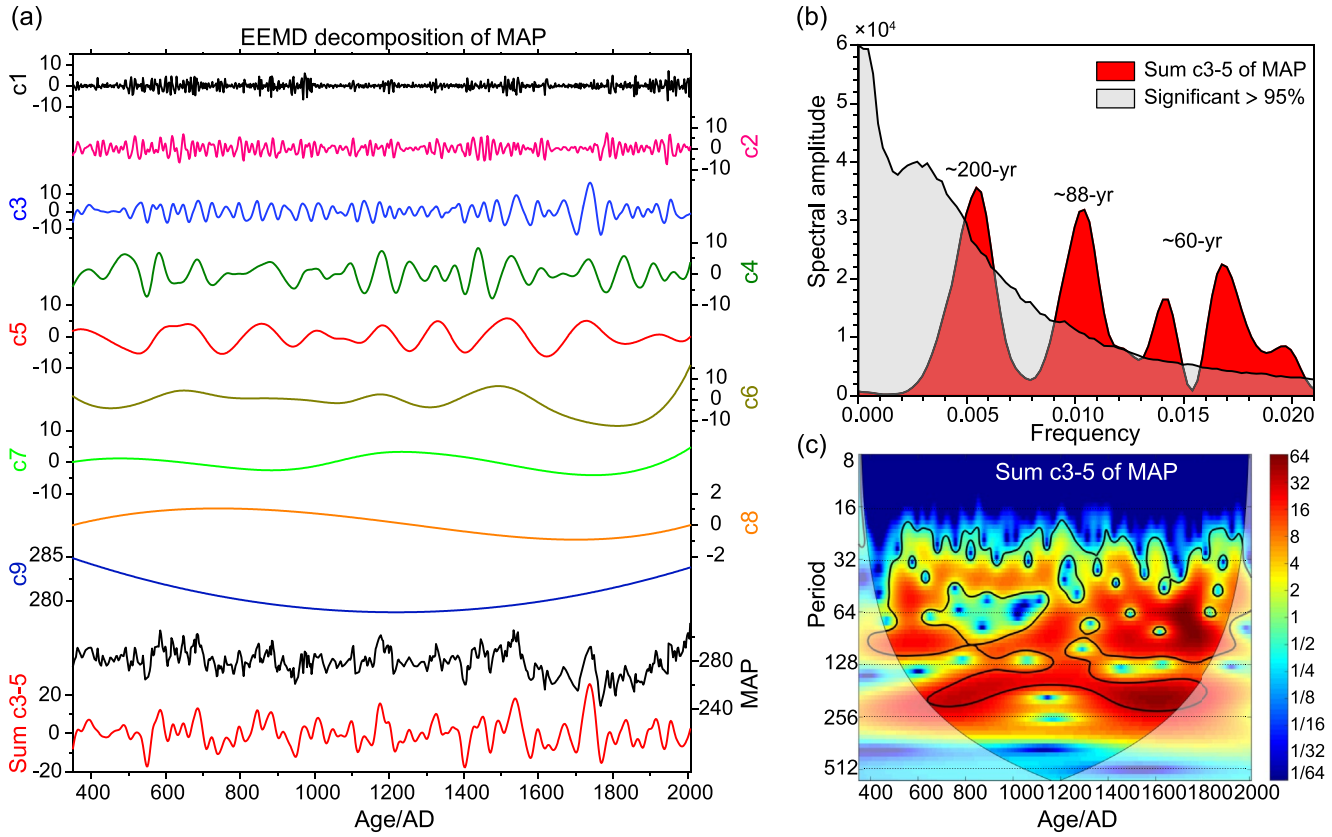

Figure 3. Results of time series analysis of the reconstructed MAP record for Kusai Lake. (a) EEMD of the reconstructed MAP. (b) Spectral analysis results of the sum of c3–5. (c) Continuous wavelet power of the sum of c3–5. EEMD, ensemble empirical mode decomposition.

To detect definite periods of dominant components, we performed spectral analysis of the detrended MAP (sum c3–5, Figure 3b). The results revealed three significant periods with central frequencies of 0.005, 0.011, and 0.017 cycles/yr, which correspond to periods of ~200-, ~88-, and ~60-years cycle, and the corresponding variances are 21%, 13%, and 12% of the total. The results of wavelet analysis (Torrence & Compo, 1998) indicate that the ~88-years and ~200-years periodic oscillations are quasi-stationary and significant during the last 1,656 years, whereas the ~60-years cycle is significant since 1200 AD (Figure 3c).

To further analyze the three periodicities, band-pass filter analysis was also performed on the sum c3–5 components of the MAP. 150–250-years band-pass filter result revealed eight ~200-years high/low precipitation oscillations, with high precipitation occurring at 450, 650, 850, 1050, 1320, 1520, 1720, and 1920 AD (Figure 4c). 80–110-years band-pass filter analysis revealed nineteen ~88-years oscillations, with high precipitation occurring at 400, 500, 580, 680, 890, 1000, 1090, 1180, 1250, 1330, 1380, 1440, 1540, 1600, 1670, 1740, 1840,1910, and 1960 AD. Interestingly, simultaneous high precipitation phases of these cycles occurred at 560–700, 890, 1160, 1330, 1440, 1540, 1740, and 1920 AD, which correspond to periods of higher Cyperaceae percentages, and are defined as coupled wet phases (Figure 2a). The high precipitation interval of 560–700 AD was mainly the result of the ~200-years cycle, while the other high precipitation intervals were mainly due to the superimposition of cycles. By contrast, simultaneous dry phases occurred at 550, 750, 950, 1400, 1580-1700, and 1750–1900 AD, which correspond to periods of higher *Artemisia* and Chenopodiaceae percentages, and are defined as coupled dry phases. The intervals of persistent low precipitation during 1580–1700 AD can be mainly attributed to the low precipitation phase of the ~200-years cycle superimposed on low-amplitude decadal cycles.

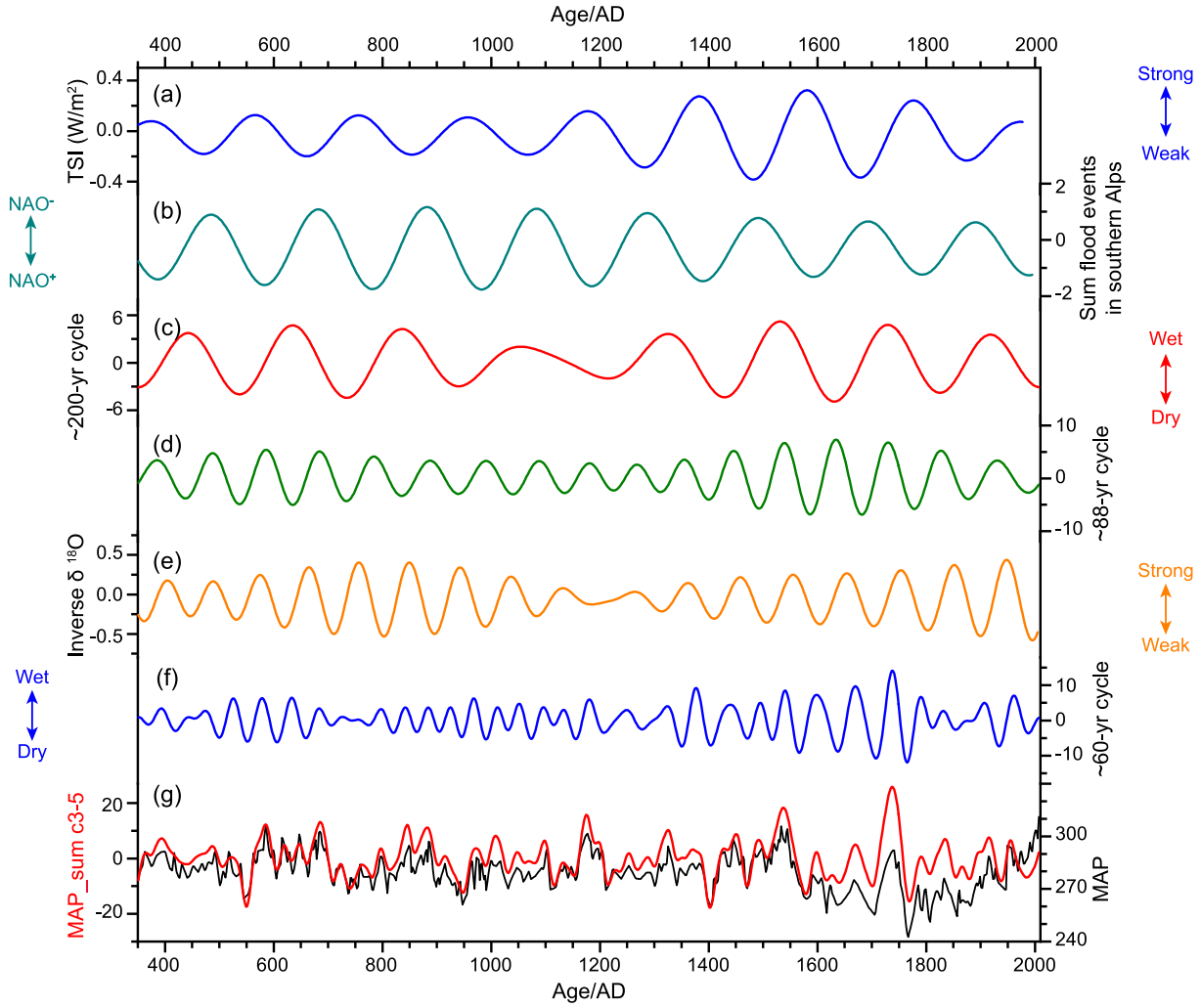

Figure 4. Comparison of cyclical changes in MAP and atmospheric circulations. 150–250-years band-pass filter result of (a) the Total Solar Irradiance (TSI), (b) the NAO phase, expressed as the sum of flood events in the Southern Alps, (c) the sum of c3–5 of MAP. 80–110-years band-pass filter result of (d) the sum of c3–5 of MAP, (e) the SASM intensity. (f) 40–75-years band-pass filter result of the sum of c3–5 of MAP. (g) The reconstructed MAP (black line) and the sum of c3–5 (red line). NAO, North Atlantic Oscillation.

4.4. MAP in the next Few Decades

The predictability of the summed c3–5 components of MAP using SSA was based on the decomposition and simulation of the time series of ~200-, ~88-, and ~60-years cycles. We first decomposed the three cycles into 50 components using SSA with the default parameters, and we then simulated the three cycles using the first 30 components. The results (Figure S6) indicate a strong correlation ($r = 0.872$, P-value < 0.001) between the reconstructed sum of c3–5 and the simulated sum of c3–5. We also predicted the MAP in the next 50 years basing on the reconstructed precipitation data for 350–1700, 350-1800, 350–1900 AD, the correlation coefficients between the reconstructed and predicted sum of c3–5 are 0.98, 0.89, and 0.85, respectively. Therefore, increasing precipitation will be expected in next few decades if these cycles are not modulated by anthropogenic forcing.

5. Discussion

The precipitation of the TP interior is closely related to variations in atmospheric circulation and is sensitive to the interaction of the Westerlies and the Asian Monsoon (Yao et al., 2013). The associations between them were established based on the backward trajectories of the source moisture for Kusai Lake,

the Westerlies transport water vapor from the remote Atlantic to the TP throughout the year, and the Asian monsoon delivers moisture from the Indian Ocean, Arabian Sea, Bay of Bengal, and South China Sea to the TP during summer (Draxler & Hess, 1997).

Our MAP record for the past 1,656-years reveals a significant ~200-years periodicity, which is also documented in paleoclimatic records from the Atlantic Ocean (Schimmelmann et al., 2003). The high/low precipitation phases of the ~200-years period in our record coincide with phases of negative/positive North Atlantic Oscillation (NAO) (Wirth et al., 2013) that can be regarded as an indicator of Westerlies intensity (Figures 4a–4c, and S7). Specifically, a negative NAO phase could enhance the Westerlies intensity and thus transport more water vapor to the TP (Wang et al., 2017a), leading to increased precipitation in the TP interior, and vice versa. Negative NAO phases in the North Atlantic corresponding to enhanced flood occurrence in the Southern Alps, and increased ice accumulation rate in the Guliya ice core (Thompson et al., 1997; Yao et al., 1996) also support this interpretation. Furthermore, the in-phase relationship and strong correlation inferred from the wavelet coherence (Grinsted et al., 2004) results between the summed record of flood events (paleo-NAO pattern) and MAP may provide evidence for the regulatory function of the NAO on the MAP across the TP interior (Figures 4, and S7). These ~200-years climatic oscillations are often attributed to variations in solar activity (Steinhilber et al., 2012).

Similarly, the high/low precipitation phases of the ~88-years periodicity in our record correspond to strong/weak phases in SASM intensity (Kathayat et al., 2017) revealed by a stalagmite $\delta^{18}O$ record from North India (Figures 4d and 4e). Contemporaneous SASM records reconstructed by tree rings and stalagmites from the SASM-influenced regions also indicate a significant periodicity around ~88-years (Figure S8), which is probably associated with the sunspot variations (Demetrescu & Dobrica, 2008). Specifically, the negative phases of the stalagmite $\delta^{18}O$ record indicate strong regional monsoon circulation, which in theory could increase the regional precipitation by regulating the amount of moisture transported from the Indian Ocean to northeastern India as well as to the TP interior. Our interpretation is supported by the results of previous studies, which suggest that enhanced moisture influx transported by the SASM was the major factor driving the increased precipitation in the TP interior (Zhang et al., 2019). However, the period of 600–1200 AD is characterized by a lagged phase relationship between SASM and MAP. The ~88-years cycle is not significant during this period, which is supported by the wavelet results (Figure 3c). The non-significance of this cycle is mainly reflected by weak or absent dry phases, indicating that precipitation over the TP interior during this period remained high even though the SASM intensity was weak.

Our results indicate that the ~60-years cyclical changes in MAP (Figure 4f) had an in-phase correlation with the Asian monsoon during 1250–2000 AD, as suggested by backward trajectories of the moisture source for Angkor in Cambodia (Buckley et al., 2010; Wang et al., 2017b, Figures S1d, and S8). This in-phase relationship can be attributed to a significant ~60-years cycle after 1200 AD (Figure 3c), which is present in both the percentages of the major pollen taxa and in MAP. The ~60-years cycle is also significantly related to El Niño-Southern Oscillation (ENSO) variability (Li et al., 2011) and the Pacific Decadal Oscillation (Shen et al., 2006b), which are coupled atmospheric circulation systems in the Pacific Ocean. Previous instrumental and paleoclimatic data have demonstrated the influences of ENSO on Asian summer monsoon rainfall (Buckley et al., 2010); an El Niño-like state could weaken the Walker circulation by producing an atmospheric motion anomaly over the Pacific and Indian Oceans, resulting in a weak Asian summer monsoon.

In summary, the influences of the mid-latitude Westerlies and the Asian monsoon on precipitation over the TP interior are complicated. Cyclical oscillations in MAP were induced by cyclical changes in the mid-latitude Westerlies and the Asian monsoon, with the mid-latitude Westerlies modulating precipitation in the form of a ~200-years cycle, and the Asian monsoon modulating precipitation in the form of multi-decadal cycles (~88-years and ~60-years). The simultaneous occurrence of wet/dry phases of these cycles could lead to a strong hydroclimatic response. For an instance, the severe drought in the 1980s AD was the result of the coincidence of dry phases (Figure 4g), which is consistent with the meteorological record. Subsequently, precipitation in the region has increased substantially because of the coincidence of the wet phases of cycles. According to the cycles in the MAP and SSA predictions for the next 50 years, the current wetting trend will continue for next few decades if these cycles are not modulated by anthropogenic forcing.

6. Conclusion

We have quantitatively reconstructed the MAP in the TP interior over the past 1,656 years based on numerical analysis of 364 fossil pollen and 735 modern pollen spectra. The MAP reconstruction revealed three significant cycles, with periodicities of ~200-, ~88-, and ~60-years, which dominated hydroclimatic variations across the TP interior. The ~200-years cycle is attributed to the Westerlies, whereas the multidecadal cycles (~60-years and ~88-years) are likely related to the Asian monsoon. The record demonstrates that precipitation variations over the TP interior were mainly controlled by the Westerlies, although the Asian monsoon made a substantial contribution in summer. The periodicities in MAP during the last 1,656 years not only support the recent humidification of the TP interior, but they also enable us to predict a possible wetting trend over next decades.

Data Availability Statement

The research data used in this study are submitted to the datasets of 4TU Center for Research Data, which will be available at https://doi.org/10.4121/13578359.v1. The data also can be temporarily downloaded from Supporting Information (Table S2).

Acknowledgments
This work was financially supported by the programs from the Chinese Academy Sciences' Project (grant nos. XDA2007010103, XDB26000000); the National Natural Science Foundation of China (grant nos. NSFC 41888101, 41830322, 41771237, 41372191), and the Yunnan Project for the Introduction of Advanced Talents (grant no. 2013HA024).

References

Braak, C. J. F. t., & Juggins, S. (1993). Weighted averaging partial least squares regression (WA-PLS): an improved method for reconstructing environmental variables from species assemblages. *Hydrobiologia*, *269*, 485–502. https://doi.org/10.1007/BF00028046

Buckley, B. M., Anchukaitis, K. J., Penny, D., Fletcher, R., Cook, E. R., Sano, M., et al. (2010). Climate as a contributing factor in the demise of Angkor, Cambodia. *Proceedings of the National Academy of Sciences of the United States of America*, *107*, 6748–6752. https://doi.org/10.1073/pnas.0910827107

Demetrescu, C., & Dobrica, V. (2008). Signature of Hale and Gleissberg Solar Cycles in the geomagnetic activity. *Journal of Geophysical Research*, *113*, A02103. https://doi.org/10.1029/2007JA012570

Draxler, R. R., & Hess, G. D. (1997). *Description of the HYSPLIT_4 modeling system, NOAA Tech. Memo. ERL ARL-224*, p. 24. Silver Spring. Retrieved from https://www.researchgate.net/publication/255682850_Description_of_the_HYSPLIT_4_modelling_system

Fick, S. E., & Hijmans, R. J. (2017). WorldClim 2: new 1-km spatial resolution climate surfaces for global land areas. *International Journal of Climatology*, *37*, 4302–4315. https://doi.org/10.1002/joc.5086

Golyandina, N., & Korobeynikov, A. (2014). Basic singular spectrum analysis and forecasting with R. *Computational Statistics & Data Analysis*, *71*, 934–954. https://doi.org/10.1016/j.csda.2013.04.009

Grimm, E. C. (1987). CONISS: A FORTRAN 77 program for stratigraphically constrained cluster analysis by the method of incremental sum of squares. *Computers & Geosciences*, *13*, 13–35. https://doi.org/10.1016/0098-3004(87)90022-7

Grinsted, A., Moore, J. C., & Jevrejeva, S. (2004). Application of the cross wavelet transform and wavelet coherence to geophysical time series. *Nonlinear Processes in Geophysics*, *11*, 561–566. https://doi.org/10.5194/npg-11-561-2004

Hou, J. Z., D'Andrea, W. J., & Liu, Z. H. (2012). The influence of ^{14}C reservoir age on interpretation of paleolimnological records from the Tibetan Plateau. *Quaternary Science Reviews*, *48*, 67–79. https://doi.org/10.1016/j.quascirev.2012.06.008

Huang, N. E., & Wu, Z. H. (2008). A review on Hilbert-Huang transform: method and its applications to geophysical studies. *Reviews of Geophysics*, *46*, RG2006. https://doi.org/10.1029/2007RG000228

Immerzeel, W. W., van Beek, L. P. H., & Bierkens, & M. F. P. (2010). Climate change will affect the Asian water towers. *Science*, *328*, 1382–1385. https://doi.org/10.1126/science.1183188

Juggins, S. (2003). *Tutorial Version. User guide: C2, Software for ecological and palaeoecological data analysis and visualization user guide version 1.3*. (13, pp. 1–24). Retrieved from https://www.researchgate.net/profile/Stephen-Juggins/publication/281600383_C2_Version_15_User_Guide/links/5fcf738e299bf188d40064a3/C2-Version-15-User-Guide.pdf

Kathayat, G., Cheng, H., Sinha, A., Yi, L., Li, X. L., Zhang, H. W., et al. (2017). The Indian monsoon variability and civilization changes in the Indian subcontinent. *Science Advances*, *3*, e1701296. https://doi.org/10.1126/sciadv.1701296

Lei, Y. B., Yang, K., Wang, B., Sheng, Y. W., Bird, B. W., Zhang, G. Q., & Tian, L. D. (2014). Response of inland lake dynamics over the Tibetan Plateau to climate change. *Climatic Change*, *125*, 281–290. https://doi.org/10.1007/s10584-014-1175-3

Li, J. B., Xie, S. P., Cook, E. R., Huang, G., D'Arrigo, R., Liu, F., et al. (2011). Interdecadal modulation of El Niño amplitude during the past millennium. *Nature Climate Change*, *1*, 114–118. https://doi.org/10.1038/nclimate1086

Liu, K. B., Yao, Z., & Thompson, L. G. (1998). A pollen record of Holocene climatic changes from the Dunde ice cap, Qinghai-Tibetan Plateau. *Geology*, *26*, 135–138. https://doi.org/10.1130/0091-7613(1998)026<0135:AAPROHC>2.3.CO;2

Liu, X. Q., Yu, Z. J., Dong, H., & Chen, H. F. (2014). A less or more dusty future in the northern Qinghai-Tibetan Plateau? *Scientific Reports*, *4*, 6672. https://doi.org/10.1038/srep06672

Lu, H. Y., Wu, N. Q., Liu, K. B., Zhu, L. P., Yang, X. D., Yao, T. D., et al. (2011). Modern pollen distributions in Qinghai-Tibetan Plateau and the development of transfer functions for reconstructing Holocene environmental changes. *Quaternary Science Reviews*, *30*, 947–966. https://doi.org/10.1016/j.quascirev.2011.01.008

Overpeck, J. T., Liu, K. B., Morrill, C., Cole, J. E., Shen, C. M., Anderson, D., & Tang, L. Y. (2005). *Holocene environmental change in the Himalayan-Tibetan plateau region: Lake sediments and the future, global change and mountain region* (pp. 83–92). Springer Netherlands.

Overpeck, J. T., Webb, T., & Prentice, I. C. (1985). Quantitative interpretation of fossil pollen spectra: Dissimilarity coefficients and the method of modern analogs. *Quaternary Research*, *23*, 87–108. https://doi.org/10.1016/0033-5894(85)90074-2

Schimmelmann, A., Lange, C. B., & Meggers, B. J. (2003). Palaeoclimatic and archaeological evidence for a ~200-yr recurrence of floods and droughts linking California, Mesoamerica and South America over the past 2000 years. *The Holocene*, *13*, 763–778. https://doi.org/10.1191/0959683603hl661rp

Schulz, M., & Mudelsee, M. (2002). REDFIT: Estimating red-noise spectra directly from unevenly spaced paleoclimatic time series. *Computers & Geosciences*, *28*, 421–426. https://doi.org/10.1016/S0098-3004(01)00044-9

Shao, X. M., Liang, E. Y., Huang, L., & Wang, L. (2005). A 1437-year precipitation history from Qilian juniper in the northeastern Qinghai-Tibetan Plateau. *PAGES News*, *13*, 14–15. https://doi.org/10.1002/joc.2143

Shen, C. M., Liu, K. B., Tang, L. Y., & Overpeck, J. T. (2006a). Quantitative relationships between modern pollen rain and climate in the Tibetan Plateau. *Review of Palaeobotany and Palynology*, *140*, 61–77. https://doi.org/10.1016/j.revpalbo.2006.03.001

Shen, C. M., Wang, W. C., Gong, W., & Hao, Z. X. (2006b). A Pacific Decadal Oscillation record since 1470 AD reconstructed from proxy data of summer rainfall over eastern China. *Geophysical Research Letters*, *33*, L03702. https://doi.org/10.1029/2005GL024804

Steinhilber, F., Abreu, J. A., Beer, J., Brunner, I., Christl, M., Fischer, H., et al. (2012). 9,400 years of cosmic radiation and solar activity from ice cores and tree rings. *Proceedings of the National Academy of Sciences of the USA*, *109*, 5967–5971. https://doi.org/10.1073/pnas.1118965109

Tang, L. Y., Mao, L. M., Shu, J. W., Li, C. H., Shen, C. M., & Zhou, Z. Z. (2016). *An illustrated handbook of quaternary pollen and spores in China*. Beijing: Science Press. Retrieved from https://www.springer.com/gp/book/9789811371028

Thompson, L. G., Yao, T. D., Davis, M. E., Henderson, K. A., Mosley-Thompson, E., Lin, P. N., et al. (1997). Tropical climate instability: The last glacial cycle from a Qinghai-Tibetan ice core. *Science*, *276*, 1821–1825.

Tian, L. D., & Yao, T. D. (2016). High-resolution climatic and environmental records from the Tibetan Plateau ice cores (in Chinese). *Chinese Science Bulletin*, *61*, 926–937.

Torrence, C., & Compo, G. P. (1998). A practical guide to wavelet analysis. *Bulletin of the American Meteorological Society*, *79*, 61–78. https://doi.org/10.1175/1520-0477(1998)079<0061:APGTWA>2.0.CO;2

Wang, S. M., & Dou, H. S. (1998). *Records of Chinese lakes*. Beijing: Science Press.

Wang, Z. Q., Duan, A. M., Yang, S., & Ullah, K. (2017a). Atmospheric moisture budget and its regulation on the variability of summer precipitation over the Tibetan Plateau. *Journal of Geophysical Research: Atmospheres*, *122*, 614–630. https://doi.org/10.1002/2016JD025515

Wang, P. X., Wang, B., Cheng, H., Fasullo, J., Guo, Z. T., Kiefer, T., & Liu, Z. Y. (2017b). The global monsoon across time scales: Mechanisms and outstanding issues. *Earth-Science Reviews*, *174*, 84–121. https://doi.org/10.1016/j.earscirev.2017.07.006

Wirth, S. B., Gilli, A., Simonneau, A., Ariztegui, D., Vannière, B., Glur, L., et al. (2013). A 2000-year long seasonal record of floods in the southern European Alps. *Geophysical Research Letters*, *40*, 4025–4029. https://doi.org/10.1002/grl.50741

Yadav, R. R. (2011). Tree ring evidence of a 20th century precipitation surge in the monsoon shadow zone of the western Himalaya, India. *Journal of Geophysical Research: Atmospheres*, *116*, D02112. https://doi.org/10.1029/2010JD014647

Yang, B., Qin, C., Wang, J. J., He, M. H., Melvin, T. M., Osborn, T. J., & Briffa, K. R. (2014). A 3,500-year tree-ring record of annual precipitation on the northeastern Tibetan Plateau. *Proceedings of the National Academy of Sciences of the USA*, *111*, 2903–2908. https://doi.org/10.1073/pnas.1319238111

Yao, T. D., Masson-Delmotte, V., Gao, J., Yu, W. S., Yang, X. X., Risi, C., et al. (2013). A review of climatic controls on $\delta^{18}O$ in precipitation over the Tibetan Plateau: Observations and simulations. *Reviews of Geophysics*, *51*, 525–548. https://doi.org/10.1002/rog.20023

Yao, T. D., Thompson, L. G., Qin, D. H., Tian, L. D., Jiao, K., Yang, Z., & Xie, C. (1996). Variations in temperature and precipitation in the past 2000 a on the Xizang (Tibet) Plateau-Guliya ice core record. *Science in China (Series D)*, *39*, 425–433.

Yao, X. J., Liu, S. Y., Sun, M. P., Guo, W. Q., & Zhang, X. (2012). Changes of Kusai Lake in Hoh Xil region and causes of its water overflowing. *Acta Geographica Sinica*, *67*, 689–698.

Zhang, C., Tang, Q. H., Chen, D. L., Ent, R. J. v. d., Liu, X. C., Li, W. H., & Haile, G. G. (2019). Moisture source changes contributed to different precipitation changes over the Northern and Southern Tibetan Plateau. *Journal of Hydrometeorology*, *20*(2), 217–229.

Zhang, G. Q., Yao, T. D., Shum, C. K., Yi, S., Yang, K., Xie, H. J., et al. (2017). Lake volume and groundwater storage variations in Tibetan Plateau's endorheic basin. *Geophysical Research Letters*, *44*, 5550–5560. https://doi.org/10.1002/2017GL073773

Zhang, L. (1992). Characteristics of temperature and rainfall distribution in the uninhabitable area Kekexili, Qinghai province (in Chinese). *Quarterly journal of applied meteorology*, *3*, 347–352.

Zhang, X. S. (2007). *Vegetation map of the People's Republic of China (1:1 000 000)*. Beijing: Geology Press. Retrieved from http://english.ib.cas.cn/Research/Achievements/200904/t20090403_1447.html

Zhao, Y., Tzedakis, C., Li, Q., Qin, F., Cui, Q. Y., Liang, C., et al. (2020). Evolution of vegetation and climate variability on the Tibetan Plateau over the past 1.74 million years. *Science Advances*, *6*, eaay6193. https://doi.org/10.1126/sciadv.aay6193